AFRL-RX-TY-TP-2010-0052

CRUMB RUBBER-CONCRETE PANELS UNDER BLAST LOADS

PREPRINT

Bryan T. Bewick
Air Force Research Laboratory
139 Barnes Drive, Suite 2
Tyndall Air Force Base, FL 32403-5323

Hani A. Salim and Aaron Saucier
University of Missouri
Columbia, MO 65211-2200
Aaron Saucier

Christopher Jackson
Applied Research Associates
P.O. Box 40128
Tyndall Air Force Base, FL 32403

Contract No. FA4819-09-C-0032

MAY 2010

AIR FORCE RESEARCH LABORATORY
MATERIALS AND MANUFACTURING DIRECTORATE

■ **Air Force Materiel Command** ■ **United States Air Force** ■ **Tyndall Air Force Base, FL 32403-5323**

REPORT DOCUMENTATION PAGE

Form Approved
OMB No. 0704-0188

PLEASE DO NOT RETURN YOUR FORM TO THE ABOVE ADDRESS.

1. REPORT DATE *(DD-MM-YYYY)*	2. REPORT TYPE	3. DATES COVERED *(From - To)*
12-MAY-2010	Journal Article PREPRINT	01-JAN-2009 -- 12-MAY-2010

4. TITLE AND SUBTITLE

Crumb Rubber-Concrete Panels Under Blast Loads

5a. CONTRACT NUMBER

FA4819-09-C-0032

5b. GRANT NUMBER

5c. PROGRAM ELEMENT NUMBER

62102F

6. AUTHOR(S)

*Bewick, Bryan T.; #Salim, Hani A; #Saucier, Aaron; **Jackson, Christopher J.

5d. PROJECT NUMBER

4918

5e. TASK NUMBER

F0

5f. WORK UNIT NUMBER

Q210FA72

7. PERFORMING ORGANIZATION NAME(S) AND ADDRESS(ES)

**Applied Research Associates, P.O. Box 40128, Tyndall Air Force Base, FL 32403
#University of Missouri, Columbia MO 65211-2200

8. PERFORMING ORGANIZATION REPORT NUMBER

9. SPONSORING/MONITORING AGENCY NAME(S) AND ADDRESS(ES)

*Air Force Research Laboratory
Materials and Manufacturing Directorate
Airbase Technologies Division
139 Barnes Drive, Suite 2
Tyndall Air Force Base, FL 32403-5323

10. SPONSOR/MONITOR'S ACRONYM(S)

AFRL/RXQF

11. SPONSOR/MONITOR'S REPORT NUMBER(S)

AFRL-RX-TY-TP-2010-0052

12. DISTRIBUTION/AVAILABILITY STATEMENT

Distribution Statement A: Approved for public release; distribution unlimited.

13. SUPPLEMENTARY NOTES

Ref AFRL/RXQ Public Affairs Case # 10-096. Document contains color images.

14. ABSTRACT

To improve the blast resistance of a wall system, it is necessary to enhance its energy absorption capabilities and/or increase its mass. Much research has been performed on improving the ductility, and thus the resistance, of a wall system using elastic materials externally attached to the tension side of a wall. This project investigated the static resistance of wall systems with elastic materials added internally to the wall system. Thus, shredded rubber is added to the concrete mix and is used to partially replace the coarse aggregates normally used in a concrete mix design. It is hypothesized that partially replacing coarse aggregates with shredded rubber is expected to improve the blast resistance of the concrete wall panels by improving its ductility. Two rubber contents were evaluated and compared to normal concrete design without any rubber. Concrete cylinders as well as full-scale concrete wall samples with coarse aggregate partially replaced with rubber were evaluated under simulated uniform loading to develop static resistance functions. Generally, it was found that the rubber reduced the compressive strength of the samples and increased the cracks that developed in the samples during testing. The maximum load and the overall resistance of the walls decreased with increasing rubber contents. Also, the failure mode for concrete samples with rubber was different from those without any rubber.

15. SUBJECT TERMS

concrete; crumb rubber; energy absorption; static resistance; blast

16. SECURITY CLASSIFICATION OF:			17. LIMITATION OF ABSTRACT	18. NUMBER OF PAGES	19a. NAME OF RESPONSIBLE PERSON
a. REPORT	b. ABSTRACT	c. THIS PAGE			Paul Sheppard
U	U	U	UU	14	19b. TELEPHONE NUMBER *(Include area code)*

Reset

Standard Form 298 (Rev. 8/98)
Prescribed by ANSI Std. Z39.18

Crumb Rubber-Concrete Panels under Blast Loads

B. Bewick[1], H. Salim[2]; A. Saucier[3]; C. Jackson[4]

Abstract: To improve the blast resistance of a wall system, it is necessary to enhance its energy absorption capabilities and/or increase its mass. Much research has been performed on improving the ductility, and thus the resistance, of a wall system using elastic materials externally attached to the tension side of a wall. This project investigated the static resistance of wall systems with elastic materials added internally to the wall system. Thus, shredded rubber is added to the concrete mix and is used to partially replace the coarse aggregates normally used in a concrete mix design. It is hypothesized that partially replacing coarse aggregates with shredded rubber is expected to improve the blast resistance of the concrete wall panels by improving its ductility. Two rubber contents were evaluated and compared to normal concrete design without any rubber. Concrete cylinders as well as full-scale concrete wall samples with coarse aggregate partially replaced with rubber were evaluated under simulated uniform loading to develop static resistance functions. Generally, it was found that the rubber reduced the compressive strength of the samples and increased the cracks that developed in the samples during testing. The maximum load and the overall resistance of the walls decreased with increasing rubber contents. Also, the failure mode for concrete samples with rubber was different from those without any rubber.

CE Database subject headings: Concrete; Crumb Rubber; Energy Absorption; Static Resistance; Blast.

Introduction

Solid waste management is one of the major environmental concerns in the world. Over 5 billion tons of non-hazardous solid waste materials are generated in USA each year. Of these, more than 270 million scrap-tires (approximately 3.6 million tons) are generated each year (Siddique and Naik, 2004). The disposal of scrap-tires is an environmental challenge facing municipalities around the world. Several studies have been carried out to reuse scrap-tires in a variety of rubber and plastic products, incineration for production of electricity, or as fuel for cement kilns, as well as in asphalt concrete. Siddique and Naik (2004) presented an overview of some of the research published regarding the use of scrap-tires in Portland cement concrete. Studies show that workable rubberized concrete mixtures can be made with scrap-tire rubber (Katib and Bayomy, 1999; Eldin and Senouci, 1993; Zheng et al., 2008; Hernández-Olivares et al., 2002; Nehdi and Khan, 2001).

Most of the research focused on the environmental favorable benefits of crumb rubber for partially replacing coarse aggregate in concrete. The improved ductility of rubberized concrete was observed by Zheng et al. (2008) by testing concrete cylinders with variable rubber contents. The brittleness index of rubber concrete samples was lower than normal concrete, which indicates that rubber-concrete samples exhibited higher ductility performance than normal concrete (Zheng et al., 2008). Eldin and Senouci (1993) concluded that rubber-concrete cylinders did not demonstrate brittle failure, but rather a ductile, plastic failure, and had the ability to absorb a large amount of plastic energy under compressive loads.

All research efforts observed reduced compressive strength and modulus of elasticity with increased rubber content in concrete. Research findings indicate

[1]Research Civil Engineer, Air Force Research Laboratory (AFRL), 139 Barnes Dr, Suite 2, Tyndall AFB, FL 32403, USA
[2] Associate Professor, University of Missouri, Columbia (MU), MO 65211-2200, USA, SalimH@missouri.edu
[3]Graduate Student, MU
[4]Research Engineer, Applied Research Associates, Tyndall AFB, FL 32403, USA

that rubber-concrete is not recommended for structural applications, but can be suitable for nonstructural purposes such as lightweight concrete walls, building facades, and architectural units (Khatib and Bayomy, 1999). Rubber-concrete mixes could also be used for transportation uses such as cement aggregate bases under flexible pavements, sound barriers, and crash barriers (Eldin and Senouci, 1993). Khatib and Bayomy (1999) also recommend that the content of rubber not exceed 20% of the total coarse aggregate content in normal concrete. In addition it was noted by Khatib and Bayomy (1999) that fine rubber crumbs produced higher compressive strength that those obtained using coarse crumb rubber.

Preliminary research by Petr (2004) indicated that rubberized concrete exhibited improved resistance to blast for panels subjected to contact detonations. Such observations and the added ductility observed from hysteresis test on cylinders (Zheng et al., 2008) and the ductile failure at ultimate of cylinders made with rubberized concrete motivated this research to investigate the blast performance of rubberized concrete panels under far-field blast loading. Therefore, the objective of this research was to evaluate the blast resistance of rubberized concrete wall panels compared to normal concrete wall panels.

In addition to the mass of the wall, the static resistance function is one of the most important properties of a wall system for resisting blast loads. The load-deflection response to failure of a wall under uniform static pressure, i.e., the static resistance function, provides the necessary information for the dynamic response prediction under blast and the energy-absorption capability of the wall system. The static resistance function also gives an insight into the modes of failure at different stages of the response.

This project experimentally evaluated the response of full-scale concrete slabs with varying rubber content partially replacing the coarse aggregate of normal concrete under simulated uniform pressure. The results allowed the determination of the failure modes and development of the static resistance functions.

Static Resistance Function

For blast design, dynamic models are used to predict the response of a structure or structural component under blast loads. Structures can be idealized and represented by a combination of springs and masses. For example, a beam or a wall that is subjected to a uniform dynamic pressure can be represented by a simple spring-mass system, shown in Fig. 1.

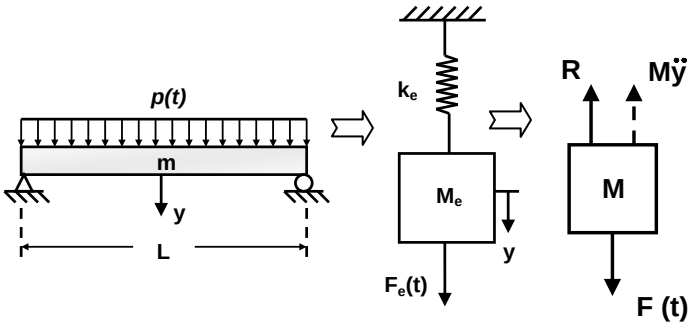

Fig. 1. Idealized SDOF spring-mass system

In order for modeling to be accurate, the idealized system must represent the actual structure. Therefore, it is important to select the proper system parameters, these being the spring constant k_e and the mass M_e. The spring constant k_e is simply the resistance of the system and can be found from the properties of the beam or wall. For complicated systems, the force-displacement relation cannot be defined by a single k_e, and thus the Static Resistance Function, R, is normally utilized. The equivalent system is chosen so that the deflection, *y*, of the concentrated mass is the same as that for some significant point on the structure, such as the midspan of a beam. The constants of the equivalent system are evaluated on the basis of an assumed deformed shape of the actual structure resulting from the static application of the dynamic loads. It is convenient to introduce certain transformation factors to convert the real system into the equivalent system. The total load, mass and resistance of the real structure are then multiplied by the corresponding transformation factors to obtain the parameters for the equivalent one-degree system. Details of this procedure can be found in Biggs (1964).

When a blast is exerted on a structure, there are many uncertainties regarding how the structure can react. In general, when a load is applied to a structure, it will travel in the path of least resistance. When an explosion takes place, pressures are placed on the outside of a building envelope, often resulting in permanent inward deflections. When modeling, this inward movement of a wall system is simplified in order to more easily predict the behavior of a system. This simplified system is commonly referred to as an SDOF model. As discussed in Biggs (1964), with this model only one type of motion is possible; or in other words, the motion of the system at any instant can be defined by a single coordinate system. For example, if the system shown in Fig. 1 is assumed to be an SDOF system, the mass could only move in a vertical direction. The first step in dynamic modeling is to isolate the mass as a free body diagram (Fig. 1), and then write an equation of motion by applying the concept of dynamic equilibrium. For Fig. 1, the equation of motion is:

$$M\ddot{y} + R - F(t) = 0$$

In this equation, Mÿ is force of inertia, R is the resistance of the spring force, F(t) is applied external force, y is displacement, and ÿ is acceleration. This differential equation can be solved to determine the variation of displacement with time once the specific parameters are defined. Thus, in predicting dynamic behavior, the static resistance of the structure or structural element must be known. Therefore, this project focuses on experimentally evaluating the Static Resistance Function of rubber-concrete, RCON, wall samples.

Fig. 2. Typical sample being tested in loading tree

Experimental Setup and Procedure

Samples were evaluated under a simulated uniform loading using a load tree. Samples were loaded at 16 points along a 3.05-m (120-in) span simply supported at both ends (Fig. 2). Displacements were measured at the quarter points along the sample and a load cell was used to measure the applied load. Samples were tested until failure and the static resistance functions were developed from the load-deflection response of the samples.

To measure displacement, three string potentiometers were connected to the sample at the quarter points. Rubber mats were placed on the samples at these points and chains wrapped around the samples. A connecting string hooked on the chain to each of the string potentiometers at each location. Cameras were installed to record testing. One camera was placed at midpoint of the samples where failure was expected and another towards the western end of the sample to observe the deformed shape of the sample during testing.

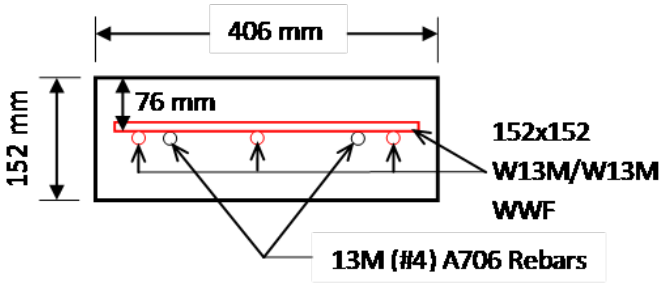

Fig. 3. Samples cross section

Test samples were cast at the Air Force Research Laboratory (AFRL) at Tyndall AFB, FL with variable content of rubber partially replacing the coarse aggregate in the normal concrete mix. Three samples were made for each of the coarse aggregate replacement variations for a total of nine full-scale wall test samples. The rubber contents were 0%, 20%, and 40% by volume of the coarse aggregate for normal concrete (Table 1). All samples were cast with the same dimensions and reinforcement. All samples were 3.66 m (144 in) long with a cross

section of 406 mm (16 in) wide by 152 mm (6 in) deep. The reinforcement consisted of one layer of 152×152 W13M/W13M (4×4 W4/W4) welded wire fabric (WWF) laid on top of two 13M (#4) A706 reinforcement bars at a depth of 76 mm (3 inches) from the tension face (Fig. 3).

Table 1. Rubberized Concrete (RCON) Test Matrix

Sample Name	Rubber Content (%)	Remarks
RCON 1	0	Cracked during shipment
RCON 2	0	Good condition
RCON 3	0	Good condition
RCON 4	20	Good condition
RCON 5	20	Good condition
RCON 6	20	Good condition
RCON 7	40	Cracked during shipment
RCON 8	40	Good condition
RCON 9	40	Good condition

Test samples were shipped while still in the casting frames from AFRL to the Remote Test Facility (RTF) at the University of Missouri. Samples were stacked during shipping and as a result two samples on the bottom cracked. RCON 1 was damaged and a crack occurred 2.13 m (84 in) measured from one end. RCON 7 developed two cracks during shipping located at 1.7 m (67 in) and 1.98 m (78 in) measured from one end.

At the RTF, the wooden forms were removed and the samples were labeled. Samples were picked up with an overhead crane and a form spreader connected to two points on the sample, each outside of quarter points on either end. The samples were placed on carts in between supports beneath the loading tree and were slid into place between supports. Bars were connected to the tree below sample creating the 16 load points across the span. Samples were then raised to support bars and carts removed.

String potentiometers were then attached to samples and checked along with cameras. Once test program was running pictures and notes were taken throughout the test. The samples were generally tested to approximately 635 mm (25 in) of deflection barring instrumentation failures. After testing was stopped, measurements of cracks were recorded.

Experimental Evaluation

The experimental program consisted of evaluating the material properties of the concrete mixes and the compressive strength of each mix (Naito et al., 2009). The static resistance function of the samples was determined experimentally using the full-scale load tree simulating static uniform pressure. In addition, observations on the failed samples were made in the form of the cracking patterns, rebar depth measurements, and unit weight measurements.

Cylinders and Mix Design

The mix design for the normal concrete was in accordance with ACI 318. The concrete mix properties for different rubber contents are given in Table 2 and Fig. 4.

Table 2. Mix Design Properties

Mix	Slump (mm)	Air Content (%)	Unit Weight (kg/m³)
0% Rubber	76	2.9	2387
20% Rubber	83	3.0	2290
40% Rubber	203	4.0	2114

Concrete cylinders were cast in 102 mm × 204 mm (4 in × 8 in) molds and allowed to cure for 28 days in accordance with ASTM C192. Three cylinders were cast for each rubber content. Compressive strength, modulus of rupture, and splitting tensile strength testing was performed according to ASTM C39, C293, and C496, respectively (Table 3). The cylinder test failure modes are shown in Figs. 5, 6, and 7. The RCON cylinders exhibited lower compressive and splitting-tensile strengths than the normal concrete. However, RCON cylinders did not display brittle failure. The RCON samples failed in a ductile, plastic manner and produced multiple fracture surfaces at ultimate. The cylinder testing results are also presented graphically in Fig. 4.

Table 3. Results of Cylinder Testing

Mix	f'_c (MPa)		f_r (MPa)	f_t (MPa)
	28 Day	79 Days		
0% Rubber	40.1	38.3	-	3.5
20% Rubber	29.9	24.5	3.7	2.2
40 % Rubber	21.3	19.3	2.9	-

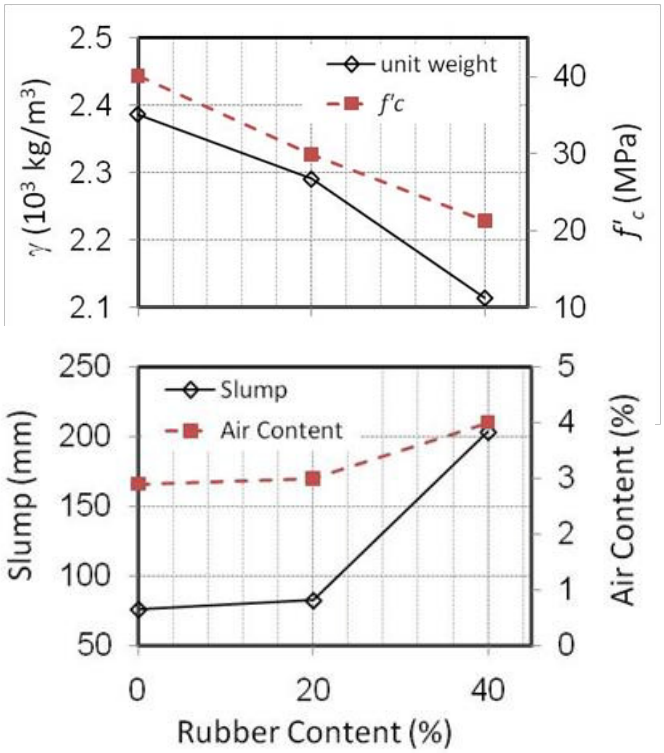

Fig. 4. Material properties degradation with increased rubber content

Fig. 5. Compressive strength testing for a 0% RCON cylinders

Fig. 6. Compressive strength testing for 20% RCON cylinders

Fig. 7. Compressive strength testing for 40% RCON cylinders

Loading Tree Testing

Control samples RCON 1–3 that contained 0% rubber developed 5 to 8 cracks within quarter points and 1 to 3 cracks outside of quarter points. Failure of the welded wire occurred first followed by compression failure in RCON 2 and 3 creating a three-hinge mechanism; however, in RCON 1 compression failure took place between two cracks near midspan during the development of a four-hinge mechanism. This was followed by a failure of the welded wire forming a hinge location resulting in a three-hinge mechanism. All RCON 0% samples experienced further compression failure and longitudinal cracking near failure cross section suggesting slip of bars in depth. In RCON 3 the rebar on the south side of the sample failed at the hinge. Tests were terminated when 635 mm (25 in) of

midspan deflection was reached with the exception of RCON 3, where the test was stopped when midspan string potentiometer disconnected at a midspan deflection of 381 mm (15 in).

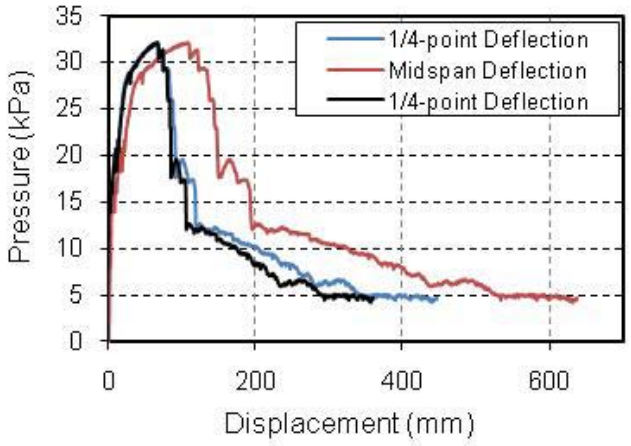

Fig. 8. Typical static response for 0% RCON samples

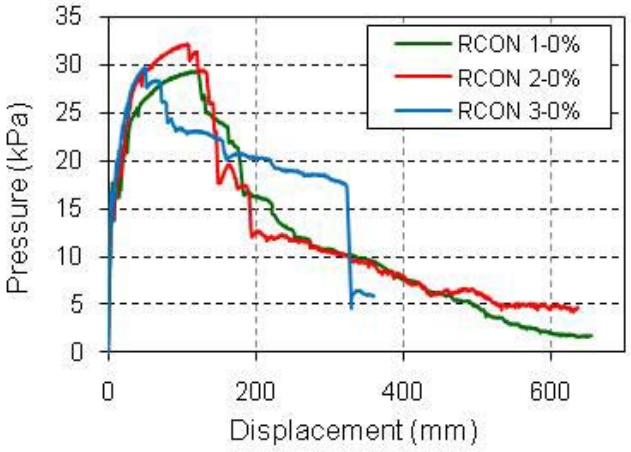

Fig. 9. Static resistance functions for control samples RCON 1-3

The pressure-deflection response of the RCON 1 – 3 samples is shown in Figs. 8 and 9. Generally, the response was linear until concrete cracking followed by a nonlinear plastic region until failure of the welded wire. This resulted in a sudden drop in the resistance followed by a flat region of plastic deformation until the concrete crushed in the compression face. The resistance then dropped gradually while longitudinal cracks developed causing the rebars to slip towards the compression face until the test was terminated. Fig. 8 shows the midspan and both ¼-point deflections for a typical 0% RCON sample. Fig. 9 shows the static resistance for the three 0% RCON samples.

Samples RCON 4 – 6 containing 20% rubber behaved similarly under uniform loading. Shortly after test started 8 to 9 cracks developed within quarter points and 2 cracks developed through pick points where form spreader was attached. RCON 5 and 6 also developed cracks through each outside quarter point. Compression failure near midspan created a three-hinge mechanism followed by welded wire failure at the hinge location. Longitudinal cracks developed near the hinge along with additional compression failure. Testing was stopped at approximately 635 mm (25 in) of deflection except for RCON 6 when testing was stopped when minimum load was reached and midspan string potentiometer disconnected.

The pressure-deflection response of the RCON 4 – 6 samples is shown in Fig. 10. Generally, the response was linear until concrete cracking followed by a bilinear plastic region until crushing failure of the compressive concrete face. This resulted in gradual drop in the resistance followed by a sudden drop due to failure of the welded wire. The resistance then dropped gradually while longitudinal cracks developed causing the rebars to slip towards the compression face until the test was terminated.

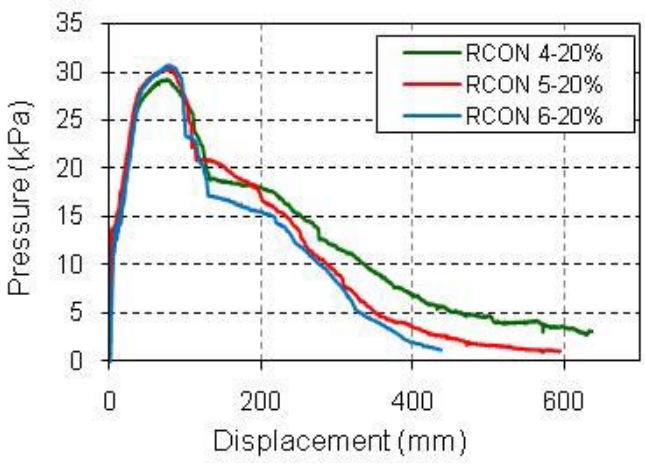

Fig. 10. Static resistance functions for 20% rubber content samples RCON 4-6

Typically, RCON 7 – 9 containing 40% rubber performed similar to 20% rubber samples. The samples developed 8 to 10 cracks within quarter points and two cracks through pick points. RCON 7, the exception, developed 3 cracks outside of quarter points and only one was through a pick point. Compression failure occurred near midspan making samples deform into three-hinge mechanisms. Welded wire failure was observed at hinge locations and samples developed longitudinal cracks near failure along with additional compression failure. The failure cross section in RCON 7 occurred at the location of the existing shipping crack. The test was stopped for RCON 7 due to minimal load, RCON 8 at 635 mm (25 in), and RCON 9 when midspan string pot ran out of travel at approximately 610 mm (24 in).

The pressure-deflection response of the RCON 7 – 9 samples is shown in Fig. 11. In general, the response was linear until concrete cracking followed by a softer linear plastic region until crushing failure of the compressive concrete face. This resulted in a sharp drop in the resistance followed by a sudden drop due to failure of the welded wire. The resistance then dropped gradually while longitudinal cracks developed causing the rebars to slip towards the compression face until the test was terminated.

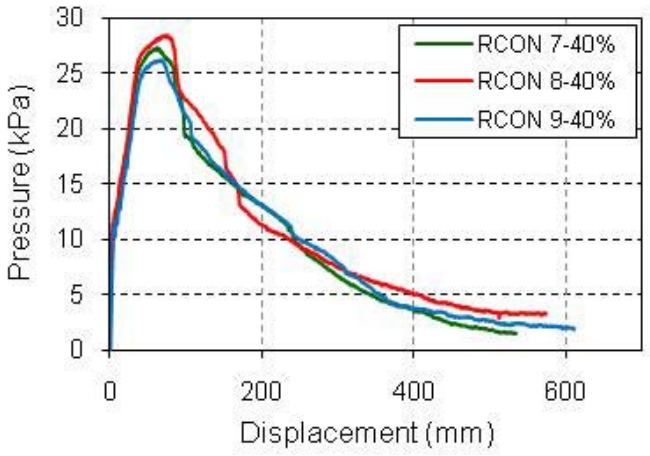

Fig. 11. Static resistance functions for 40% rubber content samples RCON 7-9

Rebar Depths

After testing, samples were cut at two locations to measure the depth of reinforcement. All depths were measured from the tension face of the sample to the center of the rebar. The rebar depths measured from the tension faces of the slabs are given in Table 4.

Table 4. Depth of Rebar and WWF in inches

	Eastern End		Western End	
Sample	**Rebar**	**WWF**	**Rebar**	**WWF**
RCON 1	2.7	2.3	2.9	2.7
RCON 2	2.8	2.6	2.8	2.6
RCON 3	2.9	2.3	2.9	2.2
RCON 4	2.6	2.4	2.5	2.2
RCON 5	2.7	2.2	2.7	2.0
RCON 6	2.7	2.1	2.7	2.2
RCON 7	2.6	2.0	2.7	2.0
RCON 8	2.5	1.9	2.7	2.3
RCON 9	2.8	2.5	2.6	2.4

Table 5. Unit Weight γ Results of Slabs

Sample	Unit Weight γ (kg/m^3)	Average γ (kg/m^3)
RCON 1	148.0	148.8
RCON 2	150.3	
RCON 3	147.9	
RCON 4	141.6	139.8
RCON 5	139.1	
RCON 6	138.7	
RCON 7	133.7	134.9
RCON 8	138.7	
RCON 9	132.4	

Unit weight

After testing, blocks were cut from RCON samples and weighed dry and submerged. The cuts were made a few inches in from the edge of the sample where there was no reinforcement. Weight measurements and calculated unit weight for the RCON samples are shown in Table 5. The higher percentage of rubber replacement correlates with lower unit weight as hypothesized and as were computed from the cylinder measurements (Table 2). Generally the unit

weights measured after testing are slightly lower than those of the cylinders (Table 2).

Load Tree Test Observations

In general for all samples, the failure cross section was near midspan at the location of a transverse welded wire. Longitudinal cracking developed close to failure after welded wire and concrete compression failure occurred. The main reinforcement bars did not fail except in control sample RCON3. Cracks in the samples were all flexural in nature; diagonal shear cracks were not observed in any of the samples.

Fig. 12 shows a typical various stages of the resistance and observed failure modes for the control samples. Initial cracking was observed near midspan followed by additional cracks within the ¼-points of the span. Concrete compression failure and development of hinge near midspan was followed by spalling of the concrete in the compression zone. Longitudinal cracks began to develop near failure cross section as the rebar began to slip towards the compression face due to catenary action developed in the rebar. A typical failed shape at test termination is a three-hinge mechanism.

The response of RCON samples with 20% and 40% rubber contents are shown in Figs. 13 and 14. Initial cracking was observed near midspan followed by additional cracks within the ¼-points of the span. The RCON samples exhibited more cracks than the control samples. Concrete compression failure and development of hinge near midspan was followed by spalling of the concrete in the compression zone. The spalling in these samples was less than the control samples, which could be attributed to the presence of the rubber fibers. Next, welded wire failed at midspan followed by longitudinal cracking. A typical failed shape at test termination is a three-hinge mechanism.

Typical static resistance functions of the RCON samples with variable rubber contents are shown in Fig.15, which indicates that the resistance decreased with increasing rubber content. The samples with higher rubber content experienced more cracking than control samples, which could be attributed to the reduced modulus of the RCON samples. In addition, as the rubber content increased, the energy-absorption capability is reduced (Fig. 16).

Fig. 15 shows the average static resistance of the RCON samples tested. The stiffness of the samples prior to first crack was reduced as the rubber content increased, whereas the stiffness of the samples after first crack was increased as the rubber content is increased. The decrease in stiffness before first crack with increased rubber content can be explained by the reduced compressive strength of the samples as shown in Table 4. On the other hand as shown in Fig. 15 and Table 6, the increase in stiffness after first crack can be attributed to the rubber shreds/fibers bridging across the cracks and slowing the crack development. The overall resistance and ultimate capacity of the RCON samples was reduced with increased rubber content (Table 6).

Spalling of the compression face was observed to be less in samples containing rubber than the control samples, whereas for the RCON samples with rubber, compression failure occurred before welded wire failure. Typically compression failure occurred in control samples before welded wire failure. The samples with rubber exhibited more transverse cracks along the span that did the control samples. This could have helped reduce the concrete stress in the compression zone. Additionally, as shown in Table 3, the compressive strength of RCON samples with rubber was less than that of the control samples. This possibly contributed to the first failure to be in compression concrete face for RCON samples 4-9.

Table 6. Resistance Comparisons

Property	Rubber Content		
	0%	20%	40%
Initial Stiffness (psi/in)	14.23	13.50	11.12
Ratio of Initial Stiffness	1.00	0.95	0.78
Plastic Stiffness (psi/in)	0.69	0.88	0.97
Ratio of Plastic Stiffness	1.00	1.27	1.41
Ultimate (psi)	4.46	4.36	3.95
Ratio of Ultimate Capacity	1.00	0.98	0.89

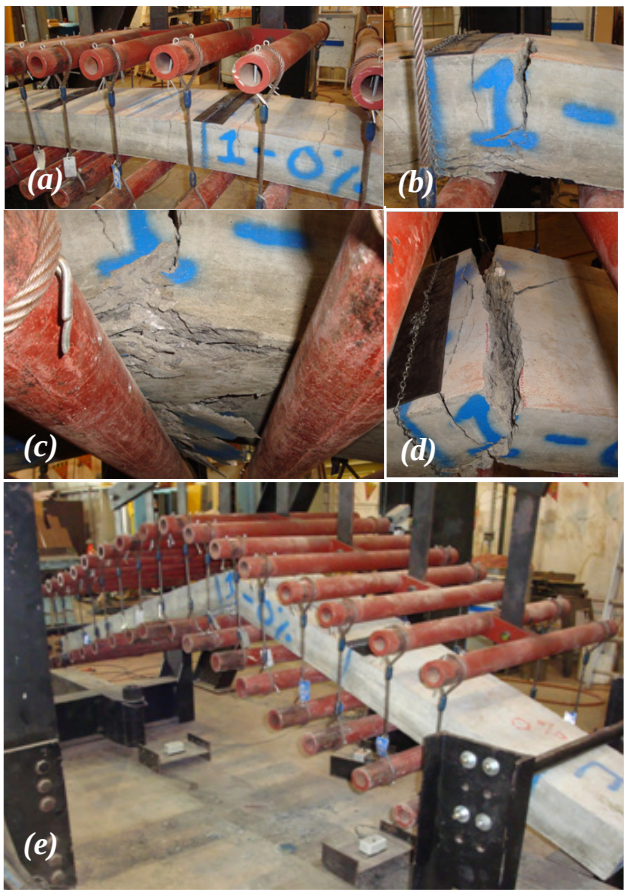

Fig. 12. Typical 0% rubber samples response: (a) initial cracking; (b) concrete compression failure near hinge; (c) spalling; (d) longitudinal cracking; (e) failed sample shape at test termination

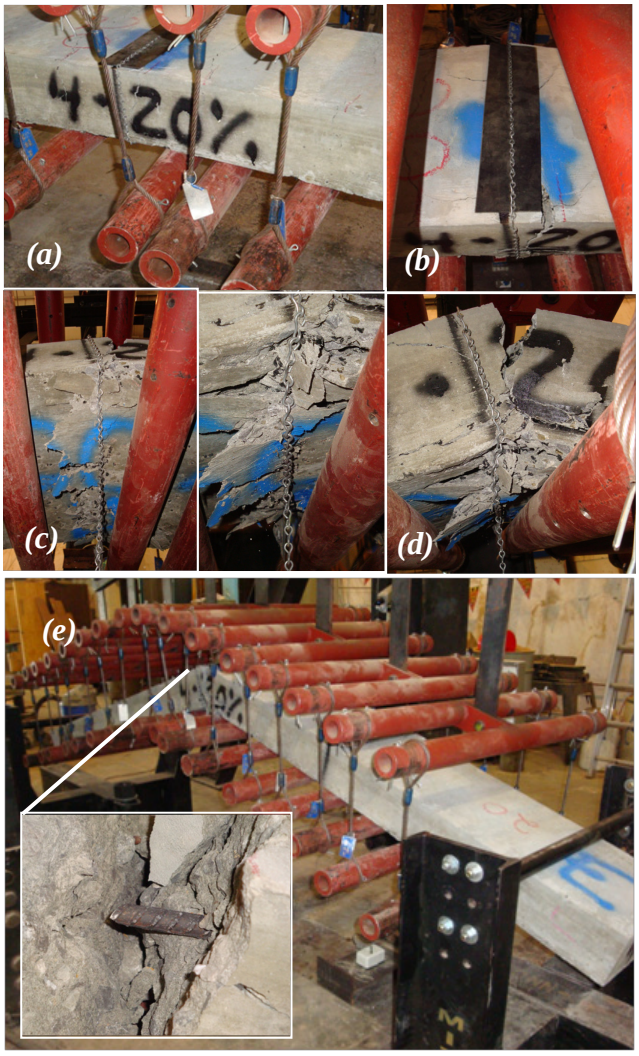

Figure 13. Typical 20% rubber samples response: (a) initial cracking; (b) longitudinal cracking; (c) spalling; (d) failure cross section; (e) failed sample shape at test termination showing rebar failure in hinge

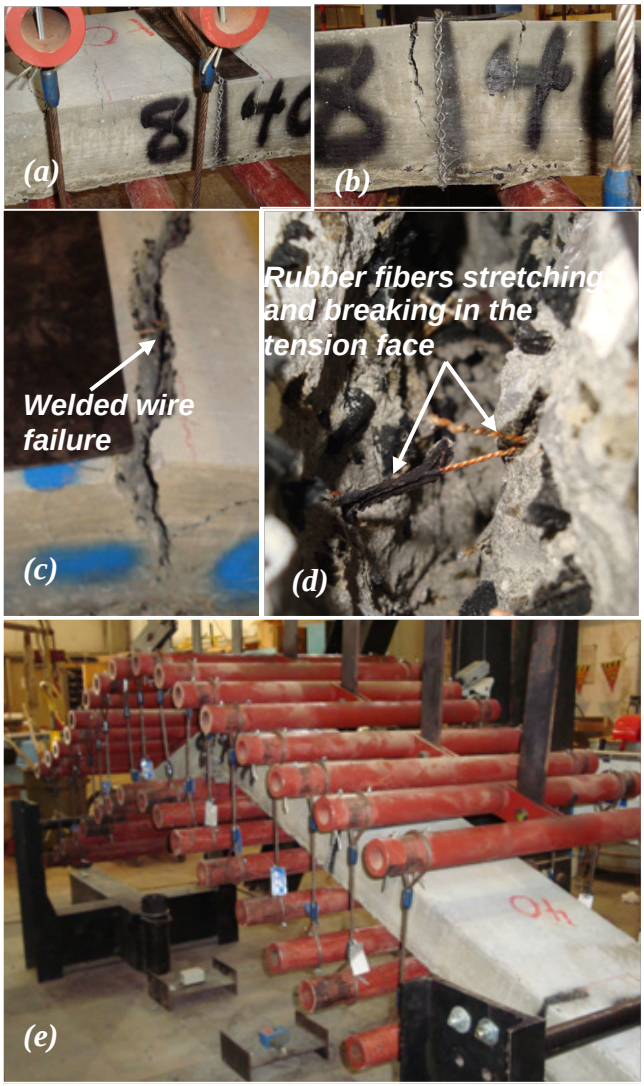

Fig. 14. Typical 40% rubber content samples response: (a) initial cracking; (b) compression failure; (c) spalling; (d) longitudinal cracking; (e), (f) and (g) failed sample shape at test termination

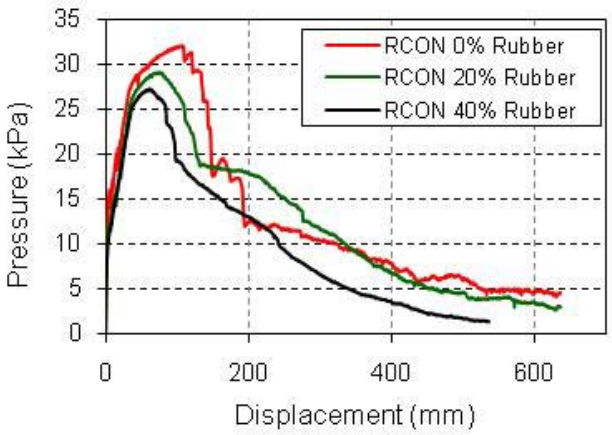

Figure 15. Typical resistance functions of RCON samples

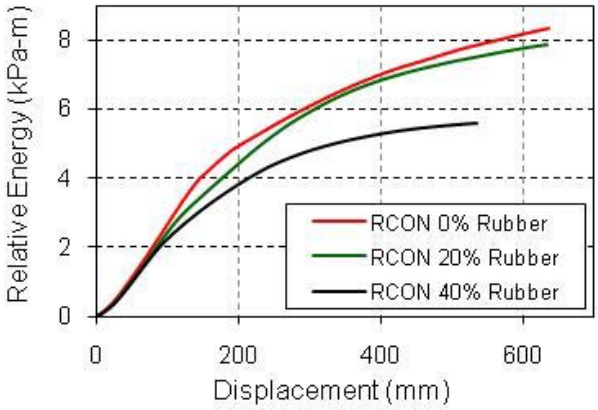

Fig. 16. Energy absorption comparison of typical RCON samples

Blast Response Comparison

The dynamic response of the RCON walls was predicted using the average static resistance functions developed in this project. The analytical response predictions were obtained by solving the equation of motion using an external explosion. The reflected blast pressure time history of a far-field explosion, which loads the wall, is normalized and shown in Fig. 17; the actual threat level and pressure values are not for public release.

The results of the dynamic response of three walls containing 0%, 20%, and 40% rubber contents under blast load are shown in Fig. 18. As the rubber content increased, the predicted normalized deflection of the walls increased, which indicates that the overall blast

resistance of the walls is reduced due to the addition of the rubber to partially replace the coarse aggregate. This result can be attributed to the reduced mass and static resistance of the walls as a result of the added rubber.

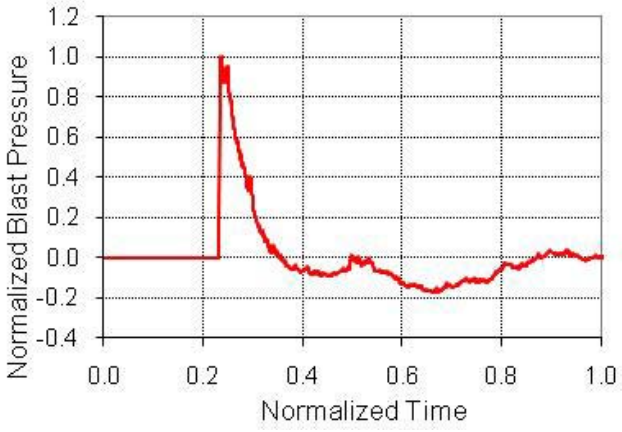

Fig. 17. Normalized reflected pressure time

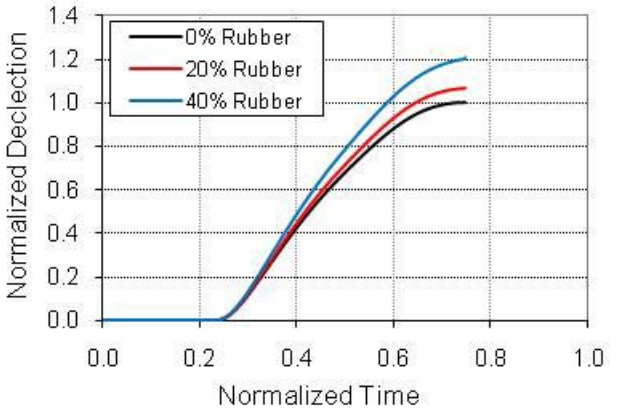

Fig. 18. Normalized dynamic response

Conclusion

This project evaluated the static resistance of wall systems with shredded rubber added to the concrete mix to partially replace the coarse aggregates in a normal concrete mix design. The compressive strength and modulus of the rubber-concrete was less than that of normal concrete without any rubber replacement. The overall static resistance of the wall samples was reduced as a result of the addition of the rubber to replace coarse aggregates of the concrete. The reduced mass and reduced resistance of the walls with rubber resulted in a reduced blast resistance. The failure mode for the concrete samples with rubber was also different from those without any rubber. The samples with rubber exhibited more cracks along the span length and produced larger stiffness after first crack developed in the sample until ultimate. The results of this study indicate that concrete walls with rubber replacement of coarse aggregates do not improve the far-field blast resistance, rather negatively impacts it when compared to normal concrete walls. It is recommended that additional testing be performed to study the effect of significant parameters that might influence the blast resistance, such as the size and shape of the rubber shreds and the use of fine rubber as a partial replacement for the fine aggregate in concrete.

References

ASTM. (2002a). *Standard test method for compressive strength of cylindrical concrete specimens. C 39/C 39 M*, West Conshohocken, Pa.

ASTM. (2002b). *Standard test method for static modulus of elasticity and Poisson's ratio of concrete in compression, C 469*, West Conshohocken, Pa.

ASTM. (2005). *Measuring ultrasonic velocity in materials, E 494*, West Conshohocken, Pa.

Eldin, N. N., and Senouci, A. B. (1993). "Rubber-tire particles as concrete aggregate." *J. Mater. Civ. Eng.*, 5(4), 478–496.

Fattuhi, N. I., and Clark, L. A. 1996. "Cement-based materials containing shredded scrap truck tyre rubber." *Constr. Build. Mater.*, 10(4), 229–236.

Hernández-Olivares, F., Barluenga, G., Bollati, M., and Witoszek, B. (2002). "Static and dynamic behaviour of recycled tyre rubber-filled concrete." *Cem. Concr. Res.*, 32, 1587–1596.

Huang, B., Li, G., Pang, S. S., and Eggers, J. (2004). "Investigation into waste tire rubber-filled concrete." *J. Mater. Civ. Eng.*, 16(3), 187–194.

Khatib, Z. K., and Bayomy, F. M. (1999). "Rubberized Portland cement concrete." *J. Mater. Civ. Eng.*, 11(3), 206–213.

Li, G., Stubblefield, M. A., Garrick, G., Eggers, J., Abadie, C., and Huang, B. (2004). “Development of waste tire modified concrete.” *Cem. Concr. Res.*, 34(12), 2293–2289.

Naito, C., Warncke, J., Jackson, C., Cotter, B., Bewick, B. (2009). *Crumb rubber concrete (CRC) performance and Design for blast and ballistic protection*, Report: AFRL-RX-TY-TR-2009-45.

Nehdi, M., and Khan, A. (2001). “Cementitious composites containing recycled tire rubber: An overviews of engineering properties and potential applications.” *Cem., Concr., Aggregates*, 23(1), 3–10.

Siddique, R., and Naik, T. R. (2004). “Properties of concrete containing scrap-tire rubber—An overview.” *Waste Manage.*, 24, 563–569.

Topçu, I. B., and Avcular, N. (1997). “Collision behaviors of rubberized concrete.” *Cem. Concr. Res.*, 27(12), 1893–1898.

Toutanji, H. A. (1996). “The use of rubber tire particles in concrete to replace mineral aggregates.” *Cem. Concr. Compos.*, 18, 135–139.

Zheng, L., Sharon Huo X., and Yuan, Y. (2008). “Strength, modulus of elasticity, and brittleness index of rubberized concrete.” *J. Mater. Civ. Eng.*, 20(11), 692-699.